UDK 544.6

NANO DIMENSION AND COBALT RATIO EFFECTS OF ACTIVE LAYER ON $LaNi_{4.3-x}Co_xMn_{0.4}Al_{0.3}$ INGOT ELECTRODES

Uong Van Vy[1], Do Tra Huong[2], Le Xuan Que[1], Nguyen Anh Tien[3]

[1] *Institute for Tropical Technology, Vietnamese Academy of Science and Technology, Hanoi, Vietnam*
[2] *Thai Nguyen City University of Education, Thai Nguyen, Vietnam*
[3] *Ho Chi Minh City University of Pedagogy, Ho Chi Minh City, Vietnam*

Поступила в редакцию 20.04.2011 г.

Abstract. Ingot electrodes have been made of blocks of $LaNi_{4.3-x}Co_xMn_{0.4}Al_{0.3}$ ($x=0 \div 1$) materials which were fabricated in an arc melting furnace and following by annealing at 1100 °C in argon atmosphere during 7 days. Surface and performance capacities of the ingot electrodes have been determined using cyclic voltammetry (CV), potentiostatic (PS) and galvanostatic (GS) techniques. Basing on the experimental data, the thicknesses of active layer (λ_a) and of performance layer (d_p) on the electrodes have been calculated. Thickness of layers depend on Co ratio in the alloys. With x Co ratio in the range from 0.5 to 0.75, the highest surface capacity, $\lambda_a = 0.4$ nm, has been considered, corresponding to two atomic layers. The performance thickness of ingot electrodes in the range from 0.8 to 1.5 μm, the highest about 2 μm was found in sample with $x = 0.75$.

Keywords: rare earth compounds, hydrogen storage materials, ingot electrodes, active layer.

INTRODUCTION

In the recent years hydride materials have become increasingly important because of their widespread application in hydrogen storage materials and batteries. The $LaNi_5$-typed alloys have absorbtion ability large quantities of hydrogen in temperature and pressure ambient. The material has recently proven to be very attractive as a negative electrode material for the rechargeable nickel-metal hydride (Ni-MH) batteries [1, 2].

The $LaNi_5$ alloy can absorb up to 5.5 H/f.u. at room temperature. An advance in $LaNi_5$-type materials is they exhibit low hysteresis, tolerant to gaseous impurities and are easily hydrogenated in the initial cycles after manufacture. Properties of the materials can be modified substantially by alloy composition, to obtain the desired storage characteristics, e.g. proper capacity at a favorable hydrogen pressure [2—4].

In this study, effects of Co ratio on some electrochemical properties, in particular on the performance active layer, of $LaNi_{4.3-x}Co_xMn_{0.4}Al_{0.3}$ materials had been investigated.

EXPERIMENT PROCEDURES

Intermetallic compounds with composition $LaNi_{4.3-x}Co_xMn_{0.4}Al_{0.3}$, $x=0$, 0.25, 0.5, 0.75, and 1, were fabricated in an arc melting furnace from La, Ni, Co, Mn, and Al high purity, upper 99.9 wt %. Then the alloys were annealed at 1100 °C in argon atmosphere in a quartz ampoule during 7 days to make sure that obtained alloys are homogeneous in phase composition and to reduce internal stress, preventing crystal out of cracking. Element composition in the alloys were examined by EDS. Ingot cylinder electrode samples were made from $LaNi_{4.3-x}Co_xMn_{0.4}Al_{0.3}$ materials block, polished with 800, 1200 and 1500 sandpaper.

Electrochemical cell includes three electrodes, working electrode (WE) is ingot electrode, reference electrode (RE) is saturated calomel electrode (SCE), and counter electrode is platinum mesh. Working and counter electrodes were dipped in 6M KOH solution. The reference electrode were connected with electrolyte by a salt-bridge, intermediate vessel contains KOH solution, and KOH-bridge. All of electrochemical measurements, cyclic voltammetric (CV), potentiostatic (PS) and galvanostatic (GS), were carried out on AUTOLAB PG.STAT 30 electrochemical system. In CV studies, scan rate variation from 5 mV/s to 1000 mV/s has been applied, the range of potential has been defined from open circuit potential (E_0) to $E=-0.8$ (V/SCE) in discharging process and from E_0 to $E=-1.2$ (V/SCE) in charging process. In the PS method, constant applied potentials have been kept at –1.2(V/SCE) and –0.8 (V/SCE) in charging and discharging process, respectively. On the contrary, for the GS technique, charg-

ing current densities J_C=–2.5 mA/cm^2 and discharging J_D=1 mA/cm^2 have been applied.

RESULTS AND DISCUSSION

1. EFFECTS OF CO RATIO ON SURFACE CAPACITIES (Q_S)

A cyclic voltammogram at various scan rates are presented in Fig.1.

Experimental charge or discharge capacity $Q(v)$, calculated can be approximately defined as following equation [5].

$$Q(v) = \int i(E)\,dt = \alpha(\Delta E)\frac{1}{v} + \text{const} \qquad (1)$$

Where the term 'const' marked as Q_S is independent of scan rate v. Thus, at very high scan rates, $Q(v)$ close to Q_S, which is considered as a surface capacity [5].

Charge capacity has been calculated from the charge branch of each CV cycle, considered from E_0 down to E_{min}=–1.2 V/SCE. Analogously, calculation of discharge capacity are carried out on the discharge branches, from E_0 up to E_{max}=–0.8 V/SCE.

Fig. 2 presents an extrapolating determination of the surface capacities Q_S on the plot of capacities variation as a function of 1/v. Capacities decrease with the scan rate increase, as indicated in equation 1.

Variation of the surface charge (Q_{SC}) and discharge capacities (Q_{SD}) of ingot electrodes as a function of Co ratio is presented in Fig. 3.

As shown in the figure, Q_{SD} reached to maximum with x=0.75, the maximum Q_{SC} occurs with x=0.5. It is clear that *QS* increase rapidly with increasing of Co ratio in the range of $0 < x < 0.5$, and reach the highest values with x=0.5 ÷ 0.75 then decrease at higher Co ratio. These effects can be explained as following: (i) Ni substitution by Co causes increase lattice parameters, (ii) Owing to Co-H bond strength is smaller than that of Ni-H and (iii) hydrogenation/dehydrogenation process on samples with Co ratio x=0.5 ÷ 0.75 are more facilitated by catalytically effect of the Co.

2. EFFECTS OF CO RATIO ON PERFORMANCE CAPACITIES

By using PS and GS technique, performance capacities (Q_P) of the ingot electrodes were determined. For the PS method, constant polarization potentials E=–1.2 V/SCE and E=–0.8 V/SCE were applied in charge and discharge process, respectively. Examples of PS discharge curves are presented in Fig. 4.

In galvanostatic polarization technique, constant current densities j_C=–2.5 mA/cm^2 and j_D=1 mA/cm^2 were applied to charge and discharge process, respectively. Discharge curves at difference cycle numbers of sample with Co ratio x=0.75 are presented in Fig. 5.

It was found that discharge capacities by both PS and GS techniques increased with cycle number. Those effects can be explained owing to increase in both the activation surface area and depth of the active surface layer. Variation in discharge capacities of samples with difference in Co ratio is plotted in Fig. 6 and Fig. 7.

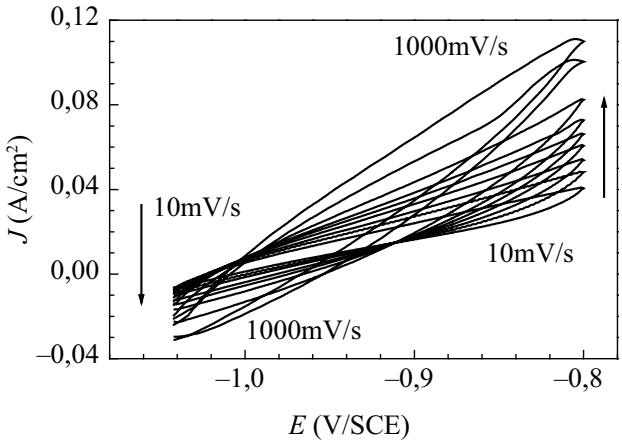

Fig. 1. Cyclic voltammogram at various scan rates in discharging process, $LaNi_{3.8}Co_{0.5}Mn_{0.4}Al_{0.3}$ ingot electrode

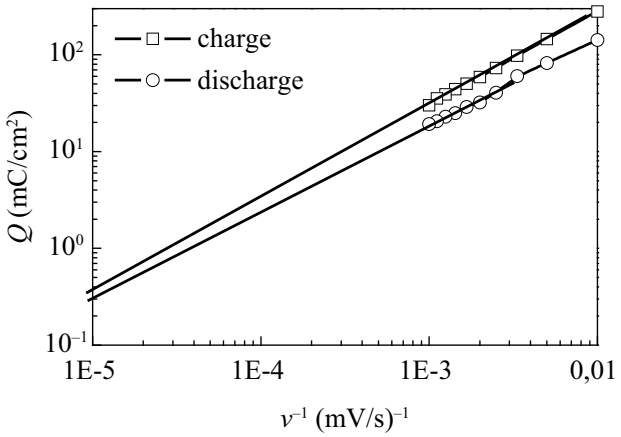

Fig. 2. Charge and discharge capacity vs. 1/scan rate plots, $LaNi_{3.8}Co_{0.5}Mn0_{0.4}Al_{0.3}$ ingot electrode

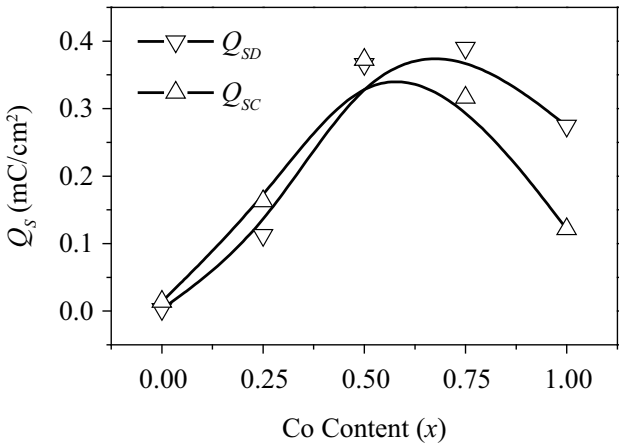

Fig. 3. Variation of Q_{SC} and Q_{SD} of ingot electrodes as a function of Co ratio x

In the Fig. 6, all curves have a bend at the 8th cycle, it can be explained as a critical value of surface capacities, where the depth of the active layer achieves a critical value which is nearly constant for the other charge — discharge cycles. Starting from 8th cycle the discharge capacities continuously increase with cycle number probably due to an increase of the active surface area and/or the depth of the active layer.

The highest critical discharge capacity about 600 mC/cm^2 were found with Co ratio $x = 0.75$. For the GS technique, the critical discharge capacities about 700 mC/cm^2 was found at Co ratio $x = 0.25$ and $x = 0.75$, is a higher than that of PS technique. This can be explained by charge — discharge force in GS technique

3. DEPTH OF ACTIVE LAYER ON THE INGOT ELECTRODE

In the charge-discharge processes, due to difficulty of H diffusion into material, rate and efficiency of hydride formation/deformation can be rise at the electrode surface region. Studying and finding out the depth of the active layer, an important technological factor, are very practically significant. In this work, the surface capacities Q_S and performance Q_p and specific properties of $LaNi_5H_6$ were used in order to calculate the depth of active surface film and of the performance layer.

Active surface film in discharge process can be called as surface hydride film. Its depth is calculated by the surface capacity at extremely high CV rate [5].

As presented in Fig.8, the depths depend strongly on the Co ratio, and the highest values of calculated depth are about 4 Å, equivalent two single atomic layers with Co ratio $x = 0.5 \div 0.75$ at both charge and discharge process.

Using PS and GS results, we can calculate the depth of the performance layer, d_p. It is necessary to note that the performance layer has a role determining the total charging/discharging capacity. Developments in its depth with PS and GS cycle numbers and Co ratio are presented in Fig. 9 and 10.

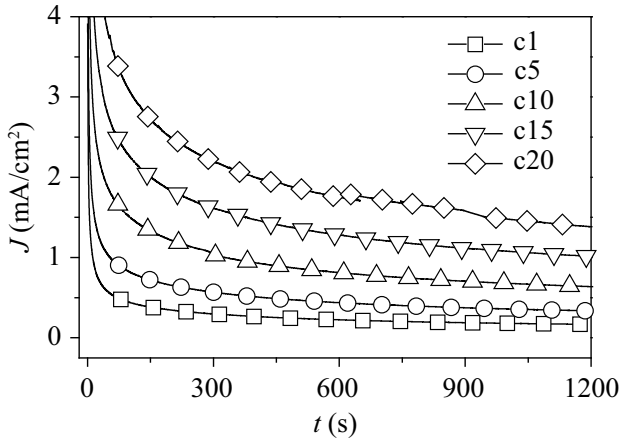

Fig. 4. Variation of discharge current densities of $LaNi_{3.55}Co_{0.75}Mn_{0.4}Al_{0.3}$ ingot electrode as a function of time and cycle number

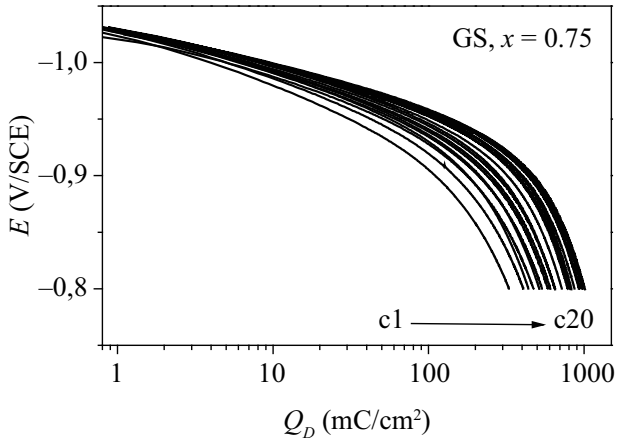

Fig. 5. Variation of discharge potential as a function of Q_D, $LaNi_{3.55}Co_{0.75}Mn_{0.4}Al_{0.3}$ ingot electrode, 1st cycle (c1) to 20th cycle (c20)

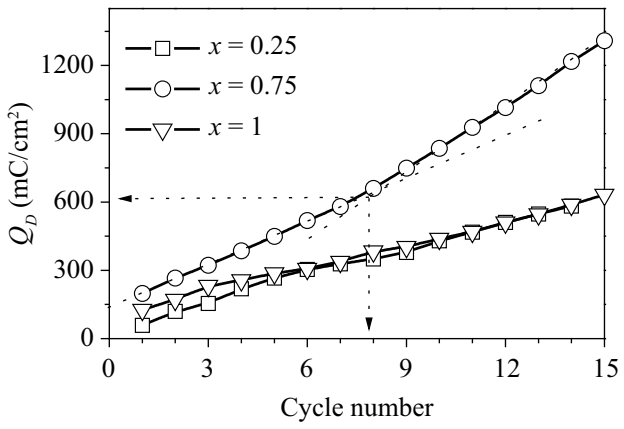

Fig. 6. Q_D variation as a function of cycle number, PS technique, Co ratio noted in the fig

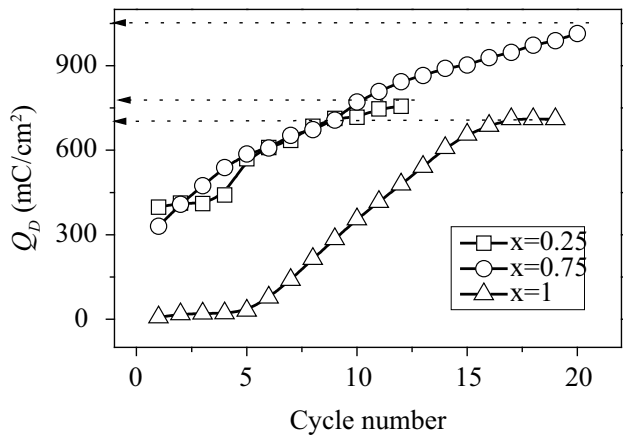

Fig. 7. Variation of Q_D as a function of cycle number, GS technique, Co ratio noted in the fig

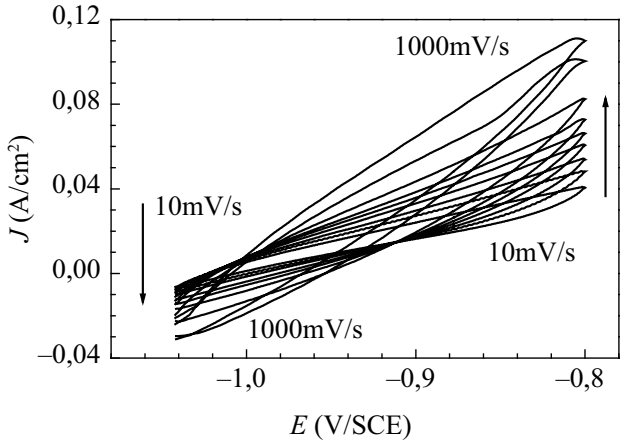

Fig. 8. Variation of the surface-active film depth as a function of Co ratio, calculated from Q_S

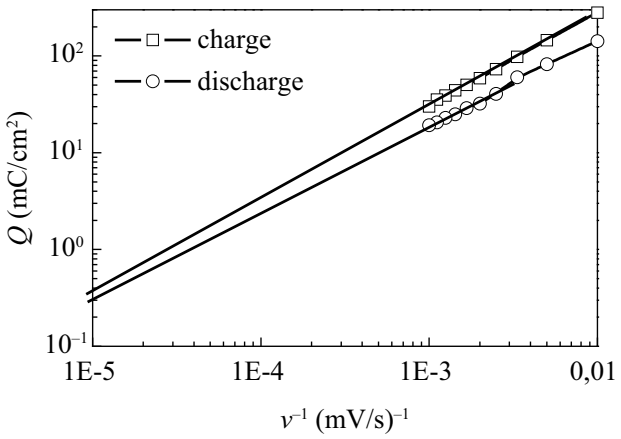

Fig. 9. Development of the performance layer depth with Co ratios and cycle number, PS technique

As can be seen, increases in the depth d_P isn't linear plot. There are bows on the curves at value of the depth about 0.8 μm (with $x=0.75$, Fig.9, $x=1.0$ Fig. 10). With $x=0.75$, this higher value, about 1.15 μm, from GS data (Fig. 10).

For the sample with Co ratio $x=1$ we can confirm that the depth of the performance layer is maximum 0.8 μm (Fig. 11), $x=0.25$ the depth is 0.85 μm, but $x=0.75$ the depth achieves 1.15 μm (Fig. 10).

From the experimental data we can divine depth of the performance layer of the ingot electrodes dtp achieves 0.8÷1.2 μm, maximum 2 μm. With Co ratio $x=0.75$, the depth achieves the highest value.

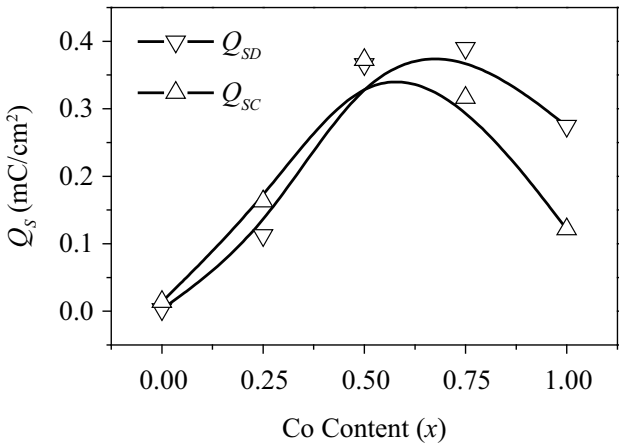

Fig. 10. Development of performance layer depth, as a function Co ratio and cycle number determined from GS data

CONCLUSION

The depths of the surface-active film λ_S can be determined using CV measurement at very high scan rates. The depth is about 4 Å corresponding to two atomic layers. All electrochemical processes on electrode have to carried out through this surface film.

The depth of the performance layer, determining total electrode charge/discharge capacity d_P calculated from GS data, achieve about 0.8÷1.5 μm, and probably maximum about 2 μm, the highest depth achieves at Co ratio $x=0.75$.

REFERENCES

1. *D. Linden and T.B. Reddy*. HANDBOOK OF BATTERIES Third Edition, McGraw-Hill 2001.

2. *P. H. L. Notten.* Rechargeable Nickel — metal hydride batteries: a successful new concept, Chapter 7, NATO ASI Series E, 1994.

3. *G. D. Adzic, J. R. Johnson, S. Mukerjee, J. McBreen and J. J. Reilly*. Journal of Alloys and Compounds, 253—254, 1997, 579—582.

4. *Le Xuan Que, Nguyen Phu Thuy*. Solid state ionics: Trends in the new millennium, 2002, 73—83.

5. *S. A. Gamboa, P.J. Sebastian, F. Feng, M. Geng and D. O. Northwood*. Journal of The Electrochemical Society, 149(2), 2002, A137-A139.

6. *M. Geng, F. Feng, J. Han, A. J. Matchett and D. O. Northwood*. International Journal of Hydrogen Energy, 26(2), 2001, 133—137.

7. *Chiaki Iwakura, Takafumi Oura, Hiroshi Inoue, Masao Matsuoka and Yoshifumi Yamamoto*. Journal of Electroanalytical Chemistry, 398 (1—2), 1995, 37—41.

8. *Jurczyk M., Majchrzycky W.* Journal of Alloys and Compounds, 311, 2000, 311—316.

Уонг Ван Ву — к.х.н., Институт тропической технологии Вьетнамской Академии наук и технологий; e-mail: uongvanvy@vnd.vast.ac.vn

Uong Van Vy — PhD, Institute for Tropical Technology, Vietnamese Academy of Science and Technology; e-mail: uongvanvy@vnd.vast.ac.vn

Ле Суан Куе — к.х.н., член-корр., доцент Института тропической технологии Вьетнамской Академии наук и технологий; e-mail: lexuanque@yahoo.com

До Ча Хыонг — к.х.н, преподаватель химического факультета Тхайнгуенского государственного педагогического университета; e-mail: dotrahuong@gmail.com

Нгуен Ань Тьен — к.х.н, преподаватель химического факультета Хошиминского государственного педагогического университета; e-mail: anhtien0601@rambler.ru

Le Xuan Que — PhD, Correspondence, associate professor, Institute for Tropical Technology, Vietnamese Academy of Science and Technology; e-mail: lexuanque@yahoo.com

Do Tra Huong — PhD, teacher, Thai Nguyen University of Education; e-mail: dotrahuong@gmail.com

Nguyen Anh Tien — PhD, teacher, Ho Chi Minh City University of Pedagogy: e-mail: anhtien0601@rambler.ru